Journal of Engineering Physics and Thermophysics, Vol. 76, No. 4, 2003

MODELING OF NATURAL THERMOGRAVITATIONAL CONVECTION IN HORIZONTAL CHANNELS WITH AN IRREGULARLY SHAPED CROSS SECTION

I. A. Ermolaev, A. I. Zhbanov, and V. S. Koshelev

UDC 536.24:532.54

Results of a numerical investigation of the natural thermogravitational convection of air in horizontal channels with a Γ-shaped cross section are presented. Two-dimensional unsteady equations of convection in the Boussinesq approximation, which are written in the velocity vortex–current function–excess temperature variables, are employed as a mathematical model. In investigating, the range of Rayleigh numbers was bounded above by the value 10^6, which corresponds to the range of applicability of the Boussinesq approximation to air in the problem posed. The boundary-value problem was solved numerically by the finite-element method of Galerkin (weak formulation). The distinctive features of the temperature and flow fields were revealed on the basis of calculations and the intensity of heat exchange was evaluated.

Introduction. Investigating convective flows in channels and tubes in the presence of the temperature differences and the gravity field, one cannot disregard, in many practical cases, the effects caused by the action of buoyancy forces. If the direction of a buoyancy force is perpendicular to the direction of a forced flow (horizontal channels), this action manifests itself as the occurrence of secondary (transverse) flow distorting the symmetry of the main flow. Secondary flow is capable of intensifying significantly heat exchange in the laminar regime [1]; however, natural convection can have an appreciable effect in the case of turbulent motion, too [2]. The influence of free convection also leads to a decrease in the length of the initial thermal portion and stimulates transition to a turbulent regime at substantially smaller Reynolds numbers.

Investigations of free-convective flows in horizontal channels with a square or rectangular cross section or a circular cross section are rather numerous [3]. Free thermoconvection in channels with a more complex geometry of the cross section has been investigated to a much lesser degree. These are usually channels with a ring-shaped cross section [4–6] or that in the form of ring sectors [7, 8]. However, triangular channels, those in the form of a sector of a circle and a regular polygon, tube bundles, and others are rather widespread. All of them can be used in systems of cooling of electronic equipment, cooling and ventilation of rooms, magnetohydrodynamic devices, in heat-exchanger elements, etc.

In works on numerical modeling of convection in complex-shaped regions, use is usually made of the control volume method (SIMPLE or SIMPLER algorithm) [9] or a combination of the grid methods and the fictitious domain method [10]. In convection problems, the method involves computation of the fictitious viscosity. However, this procedure is very laborious and time-consuming in solution of unsteady problems and it deteriorates convergence. The finite-element method enables one to naturally circumvent these difficulties.

Mathematical Model and Method of Solution. We considered two-dimensional convective flow of a viscous incompressible fluid. In solving the problem, use was made of the unsteady Boussinesq equations [11] in the velocity vortex–current function–excess temperature variables written in a Cartesian coordinate system:

$$\frac{\partial \omega}{\partial t} + U\frac{\partial \omega}{\partial x} + V\frac{\partial \omega}{\partial y} = \nu\left(\frac{\partial^2 \omega}{\partial x^2} + \frac{\partial^2 \omega}{\partial y^2}\right) + g_x \beta \frac{\partial \theta}{\partial y} - g_y \beta \frac{\partial \theta}{\partial x}, \quad (1)$$

N. G. Chernyshevskii Saratov State University, Saratov, Russia; email: ZhbanovAI@info.sgu.ru. Translated from Inzhenerno-Fizicheskii Zhurnal, Vol. 76, No. 4, pp. 134–137, July–August, 2003. Original article submitted November 1, 2002.

1062-0125/03/7604-0899$25.00

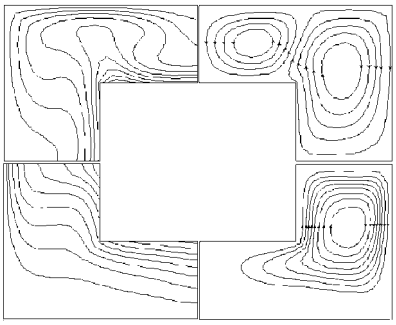

Fig. 1. Temperature fields (on the left) and flow fields (on the right) at Ra = 10^6.

$$\frac{\partial^2 \psi}{\partial x^2} + \frac{\partial^2 \psi}{\partial y^2} = \omega \,, \tag{2}$$

$$U = \frac{\partial \psi}{\partial y} \,, \quad V = -\frac{\partial \psi}{\partial x} \,, \tag{3}$$

$$\frac{\partial \theta}{\partial t} + U\frac{\partial \theta}{\partial x} + V\frac{\partial \theta}{\partial y} = a\Delta\theta \,. \tag{4}$$

The coordinate axes x and y are in parallel to the width and height of the channel cross section respectively; the channel is considered to be rather extended along the x axis. The properties of the medium were assumed to be constant except for the viscosity linearly dependent on the excess temperature.

The calculation domains represented Γ-shaped gaps (channels) between two horizontal coaxial tubes of a square cross section which were separated by longitudinal baffles (fins) (Fig. 1). The baffles were considered to be thermally thin with a negligible temperature gradient across their thickness. The Γ-shaped calculation domains (in a form of a "corner") were considered independently of one another; we also assumed the symmetry of the temperature and flow fields in the right-hand and left-hand channels relative to a vertical plane passing through the tube axis.

At the channel boundaries, we maintained the following conditions: $\theta = 0$ at the external boundaries, $q_0 = -\lambda \operatorname{grad} \theta$ (constant heat-flux density) at the internal boundaries, and $\partial\theta/\partial\mathbf{n} = 0$ on the baffles (fins). The conditions of impermeability and "sticking" $\psi = 0$ and $\partial\psi/\partial\mathbf{n} = 0$ were ensured at all the boundaries; the boundary values of the velocity vortex were computed from the Woods formula [10]. The initial conditions were $\omega = 0$, $\psi = 0$, and $\theta = 0$.

Thermoconvective flow was characterized by the following criteria: Grashof number $\mathrm{Gr} = \mathbf{g}\beta q_0 H^4/\nu^2\lambda$, Prandtl number $\mathrm{Pr} = \nu/a$ (it was set to be unity), and Rayleigh number $\mathrm{Ra} = \mathrm{GrPr}$.

In investigating convection in gases, one can expect deviations from the Boussinesq approximation (1)–(4) because of the compressibility of the gases and the high temperature coefficient of volumetric expansion. Thus, the applicability of the Boussinesq model to air is evaluated in [12]. The evaluation follows from the assumption that, in convective transfer, the thermophysical parameters change by no more than 10% as compared to the initial equilibrium state. This leads to a restriction on the temperature difference of 28.6°C, which is in agreement with [13], where the range of applicability of the Boussinesq approximation is evaluated by solving the momentum, energy, and continuity equations with allowance for the temperature dependence of the density and the thermophysical parameters. The error of the Boussinesq approximation is also investigated in [14] in the problem on free convection of air in a cavity. It is shown that the Boussinesq approximation is undoubtedly true for the maximum value of the dimensionless excess temperature $\theta'_m \le 0.1$. Furthermore, even at $\theta'_m = 0.2$ and $\mathrm{Ra} = 10^6$ the Boussinesq approximation correctly determines the Nusselt number (accurate to 2%). The correlation relation $\theta'_m = 0.0244\ \mathrm{Ra}^{0.243}$ for finding the limiting value θ'_m for which one can calculate heat exchange accurate to 5% with the use of the Boussinesq approximation is given in [14]. The investigations performed in the present work were carried out within the framework of the restrictions obtained in [14] in the range $\mathrm{Ra} = 10^3$–10^6.

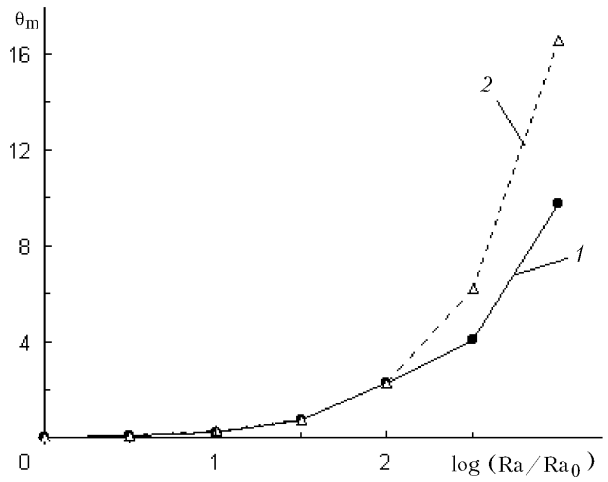

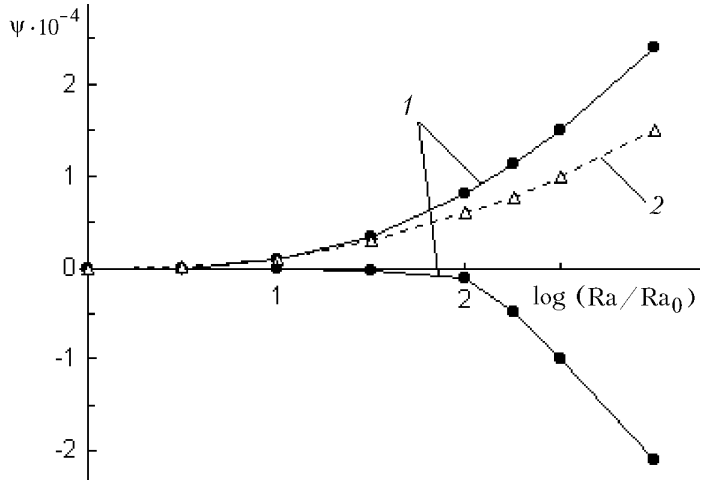

Fig. 2. Change in the maximum excess temperatures in the upper (1) and lower (2) channels with increase in the Rayleigh number.

Fig. 3. Change in the intensity of circulation of vortices (current functions) in the upper (1) and lower (2) channels with increase in the Rayleigh number.

Equations (1)–(4) were solved successively; each time step began with computation of the excess-temperature field from Eq. (4), and then we solved the equation for the velocity vortex (1) with account for (3) and the equation for the current function (2). The excess temperature, the velocity vortex, and the current function were approximated by a linear combination of time-independent basis functions (form functions) on linear triangular finite elements. The discrepancy resulting from the approximation is orthogonalized relative to the basis functions, which leads to a system of equations of the form

$$\frac{\partial}{\partial t}[C]\{\mathbf{\Phi}\} + [K]\{\mathbf{\Phi}\} + \{\mathbf{F}\} = 0 .$$

We employed the implicit time scheme for the time approximation. All the steady-state solutions were obtained by the establishment method.

Results and Discussion. The parameters of air (taken at the temperature of the exterior wall $T_0 = 0^{\circ}$C) were as follows: density $\rho = 1.293$ kg/m^3, heat capacity $c_p = 10^3$ J/(kg·K), thermal conductivity $\lambda = 0.0244$ W/(m·K), kinematic viscosity $\nu = 13.28 \cdot 10^{-6}$ m^2/sec, and temperature coefficient of volumetric expansion $\beta = 35.33 \cdot 10^{-4}$ K^{-1}. The calculations were carried out with fixed dimensions of the tube sides of 5 cm for the internal tube and 10 cm for the external tube. The thickness of the Γ-shaped gap (channel) was 2.5 cm and the height was 5 cm.

Figure 1 shows the isotherms (on the left) and the streamlines (on the right) for free-convective air flow at $Ra = 10^6$. In the upper Γ-shaped parts, flows characterized by the opposite rotation of two vortices of dissimilar intensities are formed. The convective flow results from the heating of air at the bottom and on the side; it has the form of an ascending heat jet and is the most intense near the vertical side walls. The temperature maximum is on the horizontal surface of the internal tube.

In the lower Γ-shaped parts, flows are single-vortex and they are formed in heating on the side and at the top. Flow is the most intense in the vicinity of the side walls as well; the existence of a considerable region of a nearly quiescent medium is noteworthy. The temperature maximum is at the juncture of a fin and the interior side wall. The calculations have shown that variation in the Rayleigh number in the range $Ra_0 = 10^3$–10^6 does not lead to qualitative structural changes of the flow in both the upper and lower parts.

Figure 2 shows a change in the maximum excess temperature θ_m in the upper and lower Γ-shaped channels with increase in the Rayleigh number ($Ra = 10^3$). To $Ra = 10^5$, the temperature maxima in the upper and lower parts coincide, in practice. This allows the conclusion that, to $Ra = 10^5$, heat is transferred predominantly by conduction (heat-conduction regime). When $Ra \geq 10^5$ (convective regime), more efficiently cooled are the upper parts, which is attributed to the lower maximum temperature (see Fig. 2).

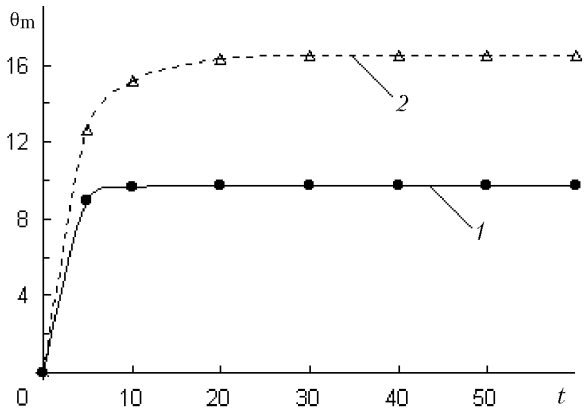

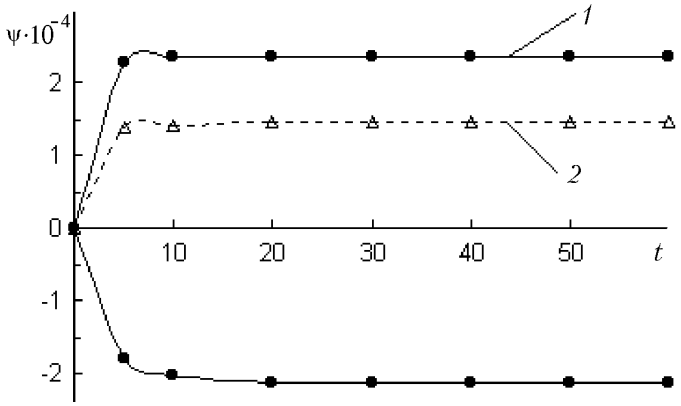

Fig. 4. Time dependences of the maximum excess temperatures in the upper (1) and lower (2) channels.

Fig. 5. Time dependences of the intensity of circulation of vortices (current function) in the upper (1) and lower (2) channels.

Figure 3 gives changes in the flow intensity (current function) of convective vortices in the upper channels (solid curves) and the vortex in the lower channels (dashed curve) with increase in the Rayleigh number. The negative values of the current function correspond to the vortex rotating in a counterclockwise direction. To Ra = 10^4, the convective flow is extremely small and flows in the upper and lower parts differ insignificantly, which confirms the conclusion of the heat-conduction regime. Above Ra = 10^5, the convective flow and heat exchange in the upper parts are much more intense than in the lower parts.

Figure 4 shows the maximum excess temperature reaching the steady-state regime for the upper (solid curve) and lower (dashed curve) channels at Ra = 10^6. Convective flow is established more rapidly in the upper Γ-shaped parts. Figure 5 shows reaching of the steady-state regime by the current functions characterizing the vortex intensity in the upper parts (solid curve) and the lower parts (dashed curve) (Ra = 10^6).

CONCLUSIONS

The results of numerical modeling of the natural convection of air in horizontal channels with a Γ-shaped cross section (in the form of a "corner") with a constant density of the heat flux at the internal boundary and a fixed temperature of the external boundary in the range of Rayleigh numbers Ra = 10^3–10^6 allow the following conclusions:

1. The structure of the temperature and flow fields in the upper and lower Γ-shaped channels have significant qualitative and quantitative differences. Two-vortex structures of flow with intense air circulation are formed in the upper channels, while lower-intensity, single-vortex flows are formed in the lower channels; there are considerable regions of a quiescent, in practice, medium.

2. A heat-conduction regime ensuring virtually the same maximum temperatures in the upper and lower channels is established to Ra = 10^5. A convective regime in which the upper Γ-shaped channels are cooled more efficiently is formed when $\mathrm{Ra} \geq 10^5$.

NOTATION

ω, velocity vortex, sec^{-1}; ψ, current function, $\mathrm{m}^2/\mathrm{sec}$; $\theta = T - T_0$, excess temperature, K; T_0, fixed temperature of the external boundary of the channel, K; x, y, z, Cartesian coordinates, m; t, time, sec; U and V, components of the velocity vector, m/sec; g_x and g_y, components of the vector of free-fall acceleration, $\mathrm{m/sec}^2$; ν, kinematic viscosity, $\mathrm{m}^2/\mathrm{sec}$; β, temperature coefficient of volumetric expansion, K^{-1}; a, thermal diffusivity, $\mathrm{m}^2/\mathrm{sec}$; q_0, heat-flux density, $\mathrm{W/m}^2$; λ, thermal conductivity, W/(m·K); **n**, vector of the external normal, m; H, characteristic dimension (height of the Γ-shaped channel), m; **g**, vector of free-fall acceleration, $\mathrm{m}^2/\mathrm{sec}$; Gr, Grashof number; Pr, Prandtl number; Ra, Rayleigh number; Ra_0, minimum Rayleigh number in the numerical calculations; θ'_m, limiting value of the dimensionless excess temperature for air to which one can employ the Boussinesq approximation [14]; θ_m, maximum excess

temperature in the numerical calculations, K; [K], stiffness matrix; [C], damping matrix; $\{\mathbf{F}\}$, element force vector; $\{\mathbf{\Phi}\}$, vector of nodal values; ρ, density, kg/m^3; c_p, heat capacity, J/(kg·K). Subscript: m, maximum.

REFERENCES

1. S. Ostrach and Y. Kamotani, *Trans. ASME, J. Heat Transfer*, No. 2, 62–68 (1975).
2. B. S. Petukhov and A. F. Polyakov, *Teplofiz. Vys. Temp.*, No. 2, 384–387 (1967).
3. O. G. Martynenko and Yu. A. Sokovishin, *Free-Convection Heat and Mass Transfer: Bibliography Guide (1797–1981)* [in Russian], Minsk, Pt. 1 (1982); Pt. 2 (1983).
4. H.-S. Law, J. H. Masliyah, and K. Nandakumar, *Trans. ASME, J. Heat Transfer*, No. 1, 115–122 (1987).
5. J. R. Custer and E. J. Shaughnessy, *Heat Conduction*, No. 4, 97–105 (1977).
6. R. E. Powe, C. T. Carley, and S. L. Carruth, *Trans. ASME, J. Heat Transfer*, No. 2, 78–87 (1971).
7. S. S. Kwong, T. Kh. Quen, and T. S. Li, *Trans. ASME, J. Heat Transfer*, No. 1, 126–134 (1981).
8. L. Iyican, Y. Bayazitoglu, and L. C. Witte, *Trans. ASME, J. Heat Transfer*, No. 4, 61–69 (1980).
9. S. Patankar, *Numerical Methods for Solving Problems of Heat Transfer and Dynamics of Fluid* [Russian translation], Moscow (1984).
10. E. L. Tarunin, *Computational Experiment in Problems of Free Convection* [in Russian], Irkutsk (1990).
11. G. Z. Gershuni, E. M. Zhukhovitskii, and A. A. Nepomnyashchii, *Stability of Convective Flows* [in Russian], Moscow (1989).
12. E. A. Spiegel and G. Veronis, *Astrophys. J.*, **131**, No. 5, 442–449 (1960).
13. J. M. Mihaljan, *Astrophys. J.*, **136**, No. 3, 1126–1131 (1962).
14. Z. V. Zhong, K. T. Yang, and J. R. Lloyd, *Trans. ASME, J. Heat Transfer*, No. 1, 135–141 (1985).